Available online at www.sciencedirect.com
ScienceDirect
Colloids and Surfaces A: Physicochem. Eng. Aspects 294 (2007) 64–70
COLLOIDS AND SURFACES A
www.elsevier.com/locate/colsurfa

On the dissolution kinetics of humic acid particles Effects of pH, temperature and Ca^{2+} concentration

Maximiliano Brigante [a,*], Graciela Zanini [b], Marcelo Avena [a]

[a] *Departamento de Química, Universidad Nacional del Sur, Av. Alem 1253, 8000 Bahía Blanca, Argentina*
[b] *CERZOS (CONICET-UNS), Departamento de Agronomía, Universidad Nacional del Sur, Bahía Blanca, Argentina*

Received 17 May 2006; received in revised form 21 July 2006; accepted 27 July 2006
Available online 3 August 2006

Abstract

The dissolution kinetics of humic acid particles has been studied in batch experiments by UV–vis spectrophotometry, and the effects of pH, temperature, stirring rate and Ca^{2+} concentrations are reported. The dissolution rate increases by more than two orders of magnitude by increasing the pH from 4 to 11 in 10^{-3} M KCl solutions. There is also an important increase in the dissolution rate by increasing temperature and stirring rate. The presence of Ca^{2+} in the electrolyte solution, on the contrary, strongly decreases the dissolution rate at constant pH. The results suggest that the increase in the dissolution rate by increasing pH is strongly related to the breaking of hydrogen bonds that hold HA molecules in the solid phase and to the increased electrostatic repulsion among negatively charged humic acid molecules. This electrostatic repulsion overcomes attractive intermolecular forces among individual molecules constituting HA particles and thus a progressive dissolution takes place. Calcium ions, on the contrary, seem to block negatively charged groups of the surface molecules reducing electrostatic repulsion. These ions may also act as bridges between functional groups of two adjacent molecules, increasing the attractive intermolecular forces.

Keywords: Solid humic acid; Humic acid–water interface; Dissolution rate; Activation energy

1. Introduction

Humic substances (HS) represent a very important and active fraction of the refractory organic matter in soils, sediments and natural waters. They result from the decomposition of plant and animal residues and they are found in all terrestrial and aquatic environments [1]. The three main fractions of humic substances are operationally defined in terms of their solubility or extractability in aqueous media as a function of pH. Humic acid (HA) is the fraction of HS that is not soluble at pH lower than around 2, but soluble at higher pH values. Fulvic acid is the fraction that is soluble in aqueous media at all pH values. Humin is the fraction of HS that is not soluble at any pH. HS are considered to be a complex mixture of different molecules of amphyphylic nature, containing different functional groups that are very active in binding metal ions, organic contaminants and mineral surfaces [2,3]. Through this binding, they may affect greatly the distribution and transport of contaminants in the environment.

HS occur in soils and sediments in several forms: (a) as dissolved molecules in the aqueous phase, (b) as adsorbed molecules or adsorbed aggregates at the surface of minerals, or (c) forming HS particles or solid aggregates [4–6]. Dissolved molecules are mobile and can be readily transported by water flows, whereas adsorbed molecules and particulate HS are less mobile and tend to be retained in the soil or sediment matrix. The effects of HS on the distribution and transport of pollutants seems to be strongly related to the ability of HS to become solubilized. In fact, whereas HS that are dissolved in water will tend to increase the mobility of the attached pollutants, HS that are forming part of the soil or sediment matrix will tend to decrease it.

Studies on adsorption–desorption, aggregation–dissagregation and precipitation–dissolution of HS are necessary to achieve a good understanding of the processes and mechanisms that result in the mobilization of these substances in aqueous media. There are many studies in the literature regarding adsorption–desorption of HS, especially HA on oxide and mineral surfaces [7–9], where the effects of pH were usually investigated. The general findings indicate that the retention of HS by solid surfaces decreases as the pH increases, which is due to a combined effect of decreased specific interactions between

* Corresponding author. Tel.: +54 291 4595101x3593
E-mail address: brigante@uns.edu.ar (M. Brigante).

0927-7757/$ – see front matter © 2006 Elsevier B.V. All rights reserved.
doi:10.1016/j.colsurfa.2006.07.045

functional groups of HS and the solid surface, and increased electrostatic repulsion between HS molecules and the solid surface and among HS molecules themselves [8]. There are also studies dealing with aggregation–dissagregation of HA [10–13]. They suggest that HA are able to form large macromolecular structures or aggregates usually at low pH in solutions of mineral acids, high ionic strengths, and high HA concentrations, due to hydrogen bonding, cation bridging and hydrophobic interactions. The attractive interactions may be disrupted by increasing the pH as a consequence of increased electrostatic repulsion among HA molecules [11,12] and also by adding simple organic acids, which form associations with HA constituting molecules [3]. Studies examining the precipitation–dissolution of HS particles were also undertaken, especially those related to their "thermodynamic" solubility in aqueous media. Indeed, the changes in solubility with pH are the basis of the operational definition of the three humic acid fractions. In addition, even though purified HA are soluble at pH > 2 by definition, it is known that HA can coagulate and precipitate at pH > 2 in the presence of metal ions [14], suggesting that an important fraction of these substances may be present in nature as precipitated HA–metal ion complexes.

Despite the studies mentioned above, dissolution kinetics of solid HS particles has not been investigated thus far. Dissolution kinetics has been very useful in the understanding of mineral weathering [15,16] and may be also useful for the case of HS. This kind of studies is needed to properly identify the conditions that promote dissolution of HS, to quantify the dissolution rates under different conditions and to assess information regarding the mobility of HS and the fate of their attached pollutants. Dissolution kinetic studies may also provide mechanistic information on the dissolution process, and fundamental information about the reactivity of the solid HS particle/water interface, topic that is gaining interest in the last years [17–19].

The aim of this article is to present a study of the dissolution kinetics of solid particles of a soil HA, which was extracted and purified according to the International Humic Substances Society (IHSS) procedures. The data obtained at a variety of pH, temperatures, stirring rates and Ca^{2+} concentrations are used to gain insights into the mechanisms that govern the dissolution process and into the factors that promote or prevent dissolution. Though the studied HA (purified sample in its protonated form) is not a product that one could encounter in nature in general, this study will be useful to gain insights into the general mechanisms involved in the dissolution of HA particles, and will serve as a basis for further studies regarding dissolution kinetics of more complex systems, such as precipitated HA–metal ion complexes.

2. Materials and methods

The HA sample used in this work was taken from an andisol (Boqueixon, A Coruña, Spain). As stated above, it was extracted and purified according to the procedures recommended by the IHSS. Its elemental composition is N (4.86%), C (52.57%), H (5.06%), O (37.18%) and S (0.33%). More information about the general characteristics of this sample, solid state ^{13}C nuclear magnetic resonance, acid–base potentiometric titrations of the HA in its dissolved state, and binding with an organic pollutant can be found elsewhere [20].

Scanning electron microscopy (SEM) was performed to investigate the size and shape of the solid HA particles, using a JEOL 35 CF microscope equipped with a secondary electrons detector. The samples were prepared on graphite stubs and coated with a ca. 300 Å gold layer in a PELCO 91000 sputter coater.

Dissolution kinetic experiments were carried out in a cylindrical, water-jacketed reaction vessel covered with a glass cap. The stirring (450 rpm in all cases except when effects of stirring rates were investigated) was controlled with an IKA RH KT/C magnetic stirrer, and carbon dioxide contamination was avoided by bubbling water-saturated N_2. The reaction temperature was maintained constant (25 ± 0.2 °C in all cases except when effects of temperature were investigated) during the experiments by circulating water through the jacket with a FAC (Argentina) water bath/circulator. Before starting a kinetic experiment, 100 mL of a 10^{-3} M KCl solution were placed in the reaction vessel, and the stirring, N_2 bubbling and water circulation were switched on. Once the temperature reached the desired value, the pH of the solution was adjusted to the desired value with KOH and/or HCl solutions. The experiment was started by adding a known weight (between 15 and 20 mg) of solid HA to the KCl solution. At different reaction times, a 5 mL aliquot was withdrawn, the particles were separated from the supernatant (by sedimentation in some cases or by centrifugation at 5000 rpm in the other cases) and the supernatant was immediately analysed to quantify the concentration of dissolved HA. After the quantification (see below), that took around 30 seconds, the supernatant and the HA particles were reintroduced into the reaction vessel. This procedure (aliquot withdrawal, separation, quantification of HA and reintroduction of the aliquot into the reaction vessel) was repeated during several hours or even days in order to achieve complete dissolution of the sample or to gather enough data points. The pH was checked periodically and kept constant by adding minute volumes of concentrated KOH or HCl solutions when necessary. In all experiments, the pH was measured with a Crison GLP 22 pH meter and a Crison 52-02 combined pH electrode.

Additional long-term dissolution experiments were performed at low pH, where dissolution was very slow. Between 15 and 20 mg of HA were placed in a centrifuge tube containing 100 mL of a 10^{-3} M KCl solution of the desired pH. The tube was then occasionally shaken, the pH controlled and readjusted if necessary, and its supernatant analysed to quantify dissolved HA. These experiments were performed at room temperature (22–26 °C) and lasted for around 3 weeks.

Quantification of dissolved HA was performed by UV–vis spectroscopy, using an Agilent 8453 UV–vis diode array spectrophotometer equipped with a Hellma 1 cm quartz cell. The supernatant of the withdrawn aliquot was placed into the cell and the spectrum was recorded in the 200–900 nm wavelength range. This equipment makes it possible to record a whole spectrum in a few seconds. Calibration curves at the working pH were constructed with several HA solutions having concentrations that ranged between 2 and 200 mg L^{-1}. The solutions were prepared

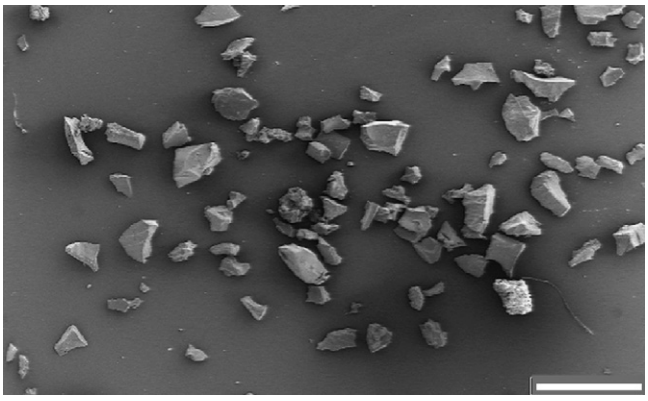

Fig. 1. SEM micrograph of the studied HA particles. The white line corresponds to a size of 1000 μm.

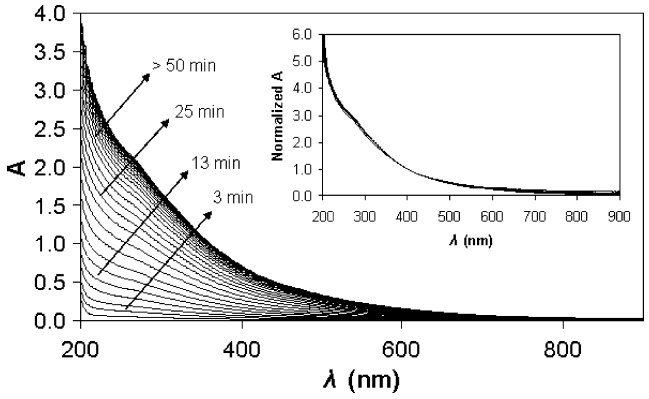

Fig. 2. UV–vis spectra of the dissolved HA at different dissolution times. pH 10 and 25 °C. The inset of the figure shows all the spectra after normalization at 400 nm.

from a concentrated solution that was obtained by completely dissolving a weighted amount of HA at pH 10 during 2 h. Very good linearity was found in all cases, at all checked wavelengths (300, 400, 500 and 600 nm) and pH values.

3. Results and discussion

Fig. 1a shows a SEM micrograph of the solid HA sample used in this study. The HA was formed by polyhedral particles whose average size was 250 μm. This relatively large size resulted in a fast sedimentation rate of the particles once they were immersed in the aqueous solution. Indeed, the sedimentation rate was so fast that in many cases, and especially at the beginning of the dissolution runs, no centrifugation step was needed to separate solid particles from the supernatant; a 20 s sedimentation step was enough for this purpose.

Each one of the HA particles seen in Fig. 1 can be regarded as a solid aggregate of molecules, which are held together by different kinds of interaction, such as hydrogen bonds, van der waals forces and hydrophobic interactions [2,5]. Due to the heterogeneous nature of HA [1,2], each particle is then a complex mixture of molecules of varying molecular weights and containing a variable amount of different functional groups (carboxylic groups, phenolic groups, aliphatic and aromatic regions, etc.). When the solid particles are immersed in a dissolving aqueous solution, their outermost molecules are readily assessable to water and dissolved ions, and thus dissolution takes place through the release of molecules to the bulk solution.

Fig. 2 shows the changes in the UV–vis spectra of the supernatant solution during a typical dissolution kinetic experiment performed at pH 10. This kind of plot was used to monitor the increase in the concentration of dissolved HA (c_{HA}) as a function of time (t) in this and all other experiments. The absorbance (A) at any wavelength increases continuously in time and eventually reaches a constant value after 50 min of reaction. The concentration of dissolved HA calculated from this constant value of A corresponded to 100% of dissolution. These results indicate that HA is gradually dissolved by the aqueous solution until complete dissolution is achieved. This last fact was also evidenced by the absence of solid particles in the reaction vessel after 50 min of reaction. The inset of Fig. 2 shows the spectra after normalization at 400 nm. All normalized spectra are coincident, except for small changes in shape that could be detected for spectra recorded at the very beginning of the dissolution run ($t < 3$ min, corresponding to less than 5% of dissolution). These small changes suggest that some humic material with a UV–vis spectrum slightly different to that of the bulk material is being dissolved at these short times. In spite of this, the small variability in spectral shapes at short reaction times and the coincidence in shapes at $t > 3$ min assure a reliable and accurate quantification of c_{HA} by UV–vis spectroscopy.

The dissolution kinetics of the studied HA can be evaluated by plotting c_{HA} as a function of t, or by plotting the degree of progress of the dissolution reaction, α, as a function of t. α is defined as

$$\alpha = \frac{c_{HA}}{c_T} \quad (1)$$

where c_T is the total concentration of HA that would be present in the dissolution vessel after complete dissolution of the solid. The magnitude of c_T can be easily calculated from the initial weight of HA and the volume of KCl solution used in the dissolution run. The value $\alpha = 0$ means that 0% of the solid has been dissolved, whereas $\alpha = 1$ means that 100% of the solid has been dissolved. A plot α versus t will be called dissolution curve.

Fig. 3 shows the dissolution curve for the data shown in Fig. 2. Dissolution was followed from the very beginning ($\alpha = 0$) to the end of the process ($\alpha = 1$). Different symbols correspond to the results obtained by using different wavelengths (300, 400, 500 and 600 nm) to quantify c_{HA}. There is a good coincidence among the curves, and thus any of these wavelengths could be used in principle to monitor the dissolution kinetics of the studied HA, in agreement with the fact that all normalized spectra are nearly coincident. From data such as those plotted in Fig. 3 the dissolution rate, R, which is defined as the slope o the dissolution curve:

$$R = \frac{d\alpha}{dt} \quad (2)$$

can be evaluated at any time. R is relatively low at the beginning of the process ($t < 10$ min), acquires its maximum value at intermediate t (12 min $< t <$ 25 min) and decreases at longer t, until

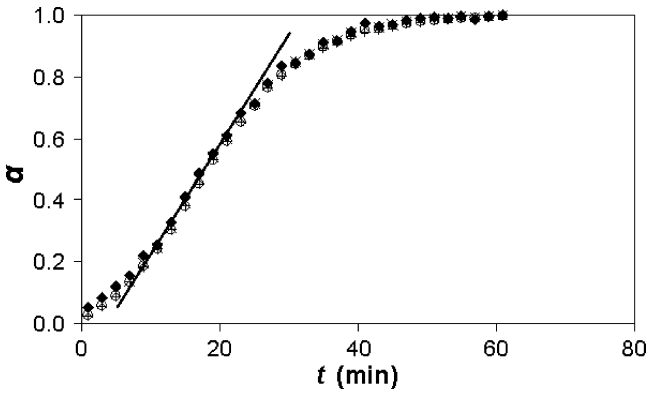

Fig. 3. Dissolution curve obtained at pH 10 and 25 °C. The four different symbols correspond to the results obtained by using different wavelengths (300, 400, 500 and 600 nm) to quantify c_{HA}. The slope of the straight line represents the maximum dissolution rate of the sample under the specified condition.

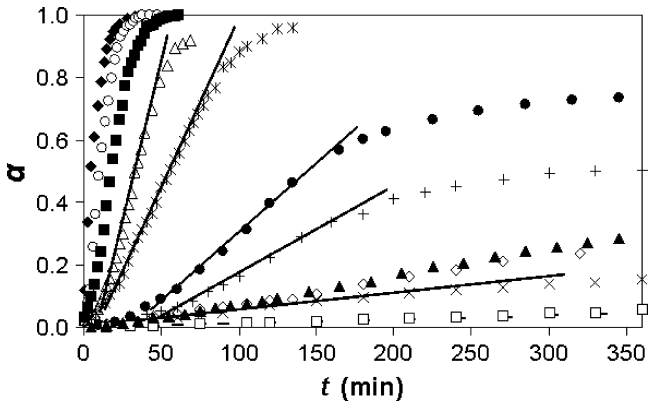

Fig. 4. Effect of pH on the dissolution curves of the studied HA at 25 °C. pH: solid diamonds, 11; open circles, 10.5; solid squares, 10; open triangles, 9.5; stars, 9; solid circles, 8.5; plus signs, 8; open diamonds and solid triangles, 7; crosses, 6; slashes, 5; open squares, 4. Note that two data sets are shown for pH 7, exemplifying the good reproducibility of the measurements. Some straight lines, whose slopes exemplify the considered dissolution rates, are also drawn in the figure.

complete dissolution is achieved. There is no clear explanation at the moment for the initial shape of the dissolution curve, which shows a relatively low dissolution rate at the beginning of the process. This low rate may be related to some slow processes that are needed before the detachment of HA molecules, such as surface hydration, or to the presence of minute amounts of cationic impurities at the surface, which slow down the dissolution process (see below). On the contrary, the shape of the curve after this initial period is rather common for dissolution kinetics of solid particles: the rate is relatively high and nearly constant during a certain time and then decreases monotonously as t increases. This is the typical behavior of solid particles whose size and surface area gradually decrease as dissolution proceeds, which is called attrition mechanism [21]. Since factors responsible for the low dissolution rate at the beginning of the process are not well understood, this period is not considered to evaluate the dissolution rate. For comparative purposes, the maximum dissolution rate observed at intermediate times is used in further analyses. For the case exemplified in Fig. 3, this rate is given by the slope of the straight line drawn in the figure.

The effects of pH on the dissolution behavior of the studied HA are shown in Fig. 4. The kinetics is strongly dependent on pH, i.e., the dissolution rate is relatively high at high pH, but decreases markedly as the pH decreases. In fact, only 30 min were necessary to produce complete dissolution of the solid at pH 11, whereas at pH 4–5 only 6% of the initial solid could be dissolved after 6 h of reaction. In addition, it can be observed that complete dissolution could be achieved in all experiments performed at pH 9 or higher, but no completeness was achieved at pH 8.5 or lower during the time that the experiment lasted. Since it has been informed in the literature that the solubility of purified HA decreases as the pH decreases [14,22], a question arises here on whether the low dissolution rate at low pH is due (i) to the intrinsic slowness of processes that lead to the detachment of HA molecules from the solid surface, or (ii) to the fact that solubility equilibrium is being reached at these low pH values, and thus some backward precipitation reaction is decreasing the net dissolution rate. An answer to the question can be given by performing long-term experiments trying to approach solubility equilibrium from dissolution and precipitation. The results of these experiments are exemplified by data in Fig. 5, which shows, on one side, the long-term dissolution behavior of the HA at pH 4, and, on the other side, the precipitation behavior of a sample whose pH was decreased to 4 after complete dissolution at pH 10. The dissolution curve shows that dissolution increases monotonously as t increases. Although the dissolution rate is very low, no signs of equilibration could be detected after three weeks of reaction. The precipitation curve, on the other hand, shows that a very fast coagulation–precipitation takes place after decreasing the pH from 10 to 4. α decreased from 1 to 0.78 in less than 10 min and then remained independent of the reaction time during the three weeks that the experiment lasted. If instead of decreasing the pH from 10 to 4, it is decreased from 10 to 7, a fast precipitation also occurs until $\alpha = 0.87$, which then becomes independent of time (data not shown). The trends of the curves in Fig. 5 suggest that during dissolution, the system is always far from the solubility equilibrium under our exper-

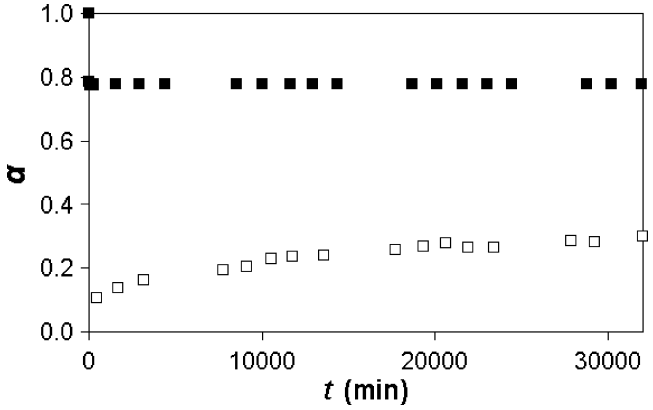

Fig. 5. Long-term dissolution–precipitation experiments at 25 °C. Open symbols show the dissolution curve of the studied HA sample at pH 4. Solid symbols show the precipitation behavior of a sample whose pH was decreased to 4 after complete dissolution at pH 10. $t = 0$ in the precipitation curve corresponds to the moment of the addition of HCl solution to decrease the pH from 10 to 4.

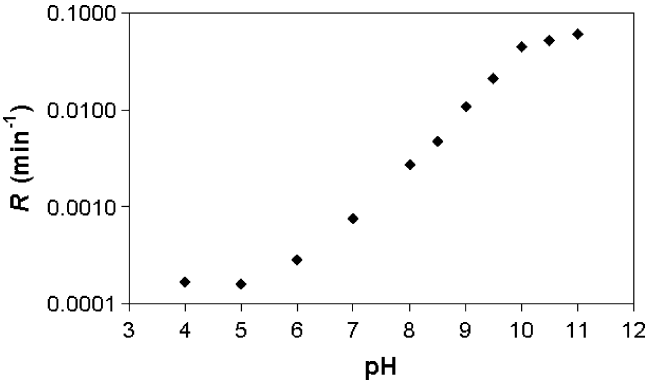

Fig. 6. Effect of pH on the dissolution rate of the studied sample at 25 °C.

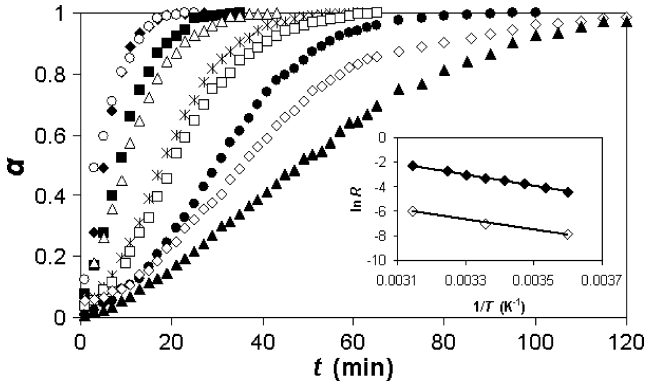

Fig. 7. Effect of temperature on the dissolution curves of the studied HA at pH 10. Solid diamonds, 45 °C; open circles, 40 °C K; solid squares, 35 °C; open triangles, 30 °C; stars, 25 °C; open squares, 20 °C; solid circles, 15 °C; open diamonds, 10 °C; solid triangles, 5 °C. The inset of the figure shows the linearized plots of Arrhenius equation for data obtained at pH 10 (solid diamonds) and pH 7 (open diamonds). Dissolution curves at different temperatures and pH 7 are not shown.

imental conditions. Therefore, it seems that the low dissolution rate at low pH is because of the slowness of the process that lead to the detachment of HA molecules from the solid surface, and not because solubility equilibrium is being reached.

The strong pH dependency of the dissolution rate can be better observed by plotting the logarithm of the dissolution rate as a function of pH, which is shown in Fig. 6. Maximum dissolution rates (slope of straight lines in Fig. 4) were used for comparative purposes. The rate increases by more than two orders of magnitude (400-fold increase) from pH 4 to 11. Most of the variations take place between pH 5 and 10. Unfortunately, there are no data in the literature regarding the dissolution kinetics of HA to compare with data presented here. In spite of this, the results are comparable to those reported by Avena and Wilkinson [11] for the disaggregation kinetics of soluble and relatively small (hydrodynamic radius of about 300 nm) aggregates of a purified peat HA. According to these authors, the disaggregation rate increased by more than three orders of magnitude from pH 3.6 to 5.6. Although somewhat different to the case of dissolution of solid HA particles, disaggregation is also a dynamic process where molecules are detached from aggregates and released to the bulk solution, and thus results should be somewhat comparable.

Dissolution of solid particles in aqueous media usually proceeds in several steps [23], such as (1) mass transfer of dissolved reactants (e.g., protons or hydroxyl ions), (2) reactions of these reactants with molecules or ions located at the solid surface, and (3) mass transfer of the reaction products into the bulk solution. Any one or more of these steps can be rate-controlling, but it is customary to identify the kinetic processes as either transport-controlled processes (where step (1) or (3) is the rate-limiting step) or surface-controlled processes (where one or more of the reactions involved in step (2) are the rate-limiting steps). As stated by Lasaga [24], both cases are only appropriate as extreme limiting cases, and often the rate is a more complex function of both the transport and the surface kinetics. Effects of temperature and stirring rate often give some clues that help to decipher what the dominant mode (if any) of dissolution is. Strong temperature effects normally indicate surface-controlled dissolution because these effects are relatively weak for diffusion in aqueous media. In addition, because stirring rate influences the transport rate of species in solution, absence of stirring rate effects is also a good indicator of surface-controlled dissolution [24].

The effects of temperature on the dissolution curves at pH 10 are shown in Fig. 7. The rate significantly increases as temperature increases. The apparent activation energy (E_{app}) for the dissolution process was 38 kJ mol^{-1} (inset of Fig. 7), as calculated by using Arrhenius equation

$$R = A \exp\left(-\frac{E_{app}}{RT}\right) \quad (3)$$

where A is the Arrhenius pre exponential term. The same kind of experiment, but at pH 7, yielded a value of 35 kJ mol^{-1} (inset of Fig. 7), showing that E_{app} does not vary significantly with the pH. Sparks [23] indicates that typical values of E_{app} are <21 kJ mol^{-1} for transport-controlled processes in water and 42–84 kJ mol^{-1} for surface processes controlled by chemical reactions at solid surfaces. Intermediate values may be found for mixed-control (transport and surface) of the dissolution reaction [21]. It must be noted that the range 42–84 kJ mol^{-1} has been established for dissolution of minerals, and may not apply strictly to the dissolution of HA particles. The relatively high values of E_{app} deduced from Fig. 7 indicate that HA dissolution is not purely controlled by transport processes in water. These values are very close to those corresponding to surface-controlled processes, suggesting that surface reactions are playing an important role in the dissolution kinetics. However, since apparent activation energies are within the range usually attributed to mixed-control, some participation of transport in the kinetic control cannot be ruled out. In fact, dissolution kinetic studies performed at different stirring rates (between 150 and 600 rpm, data not shown) showed that the dissolution rate increases linearly with the stirring rate ($r^2 = 0.996$). Therefore, the combined analysis of temperature and stirring rate effects indicates that there is a mixed-control of the dissolution kinetics under our experimental conditions.

Besides attractive forces that tend to keep HA molecules together in a solid particle, electrostatic repulsive forces may also operate among the molecules, since carboxylic and phenolic functional groups become negatively charged upon deprotonation. For the case of HA molecules in aqueous solutions,

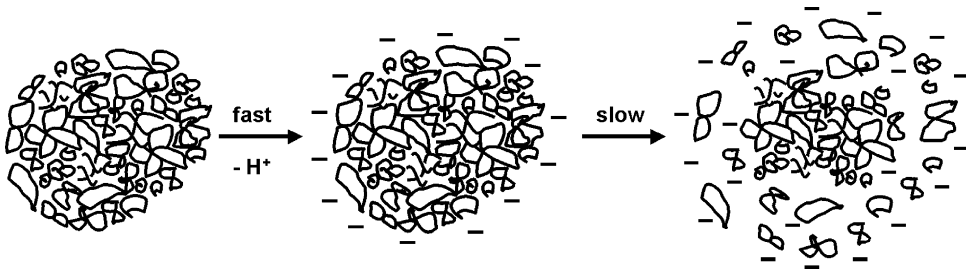

Fig. 8. Schematic representation of the mechanism proposed for the dissolution of HA particles.

carboxylic groups deprotonate at pH around 4 or 5 and phenolic groups deprotonate at pH around 9 or 10 [25]. This gives rise to a continuous increase in the negative charge as the pH increases, until pH above 10 or 11 where charge versus pH curves become flatter. A similar charging behavior should take place in HA molecules in the surface of a solid particle, even though some differences could be expected as a result of the different environment in which surface molecules are located as compared to dissolved molecules. In addition, deprotonation of carboxylic and phenolic groups may cause the breaking of some hydrogen bonds that contribute to hold the HA molecules together in the solid. The release of protons involved in these bonds could leave the surface molecules more susceptible to detachment. Therefore, it is possible to speculate that the main effects of increasing pH on the dissolution rate are due to an increased concentration of molecules susceptible to detachment at the solid surface, and to an increased electrostatic repulsion among these surface molecules. The results can be resumed in a schematic two-step mechanism for dissolution of HA, which is presented in Fig. 8. The left-hand-side drawing represents a solid HA particle formed by many HA molecules. Once immersed in an aqueous solution, a rather fast deprotonation process takes place, leading to the breaking of hydrogen bonds and the development of negative charges on the molecules located at the surface of the particle. These processes eventually induce the detachment of the surface molecules and the progressive dissolution of the material. A similar mechanism was proposed to explain the dissagregation behavior of a purified peat HA [11]. Electrostatic repulsion among the molecules was also suggested as a very important factor affecting the desorption rate of HA from mineral surfaces [8], and affecting the coagulation–precipitation behavior of HA molecules [14].

Fig. 9 shows the effects of Ca^{2+} concentration on the dissolution curves of HA, which were obtained in 10^{-3} M KCl solutions to which different amounts of $CaCl_2$ were added. There is an important decrease in the dissolution rate as the concentration of Ca^{2+} increases. Although it is known that calcium ions can promote coagulation and precipitation of humic acids [14], it must be remarked that the system was always far from solubility equilibrium in our experimental conditions. In fact, the addition of Ca^{2+} up to a concentration equal to 10^{-3} M to a previously dissolved HA sample did not produce any coagulation or precipitation, indicating that the system was always undersaturated with respect to coagulation-precipitation. These results are in agreement with those informed by Weng et al. [14],

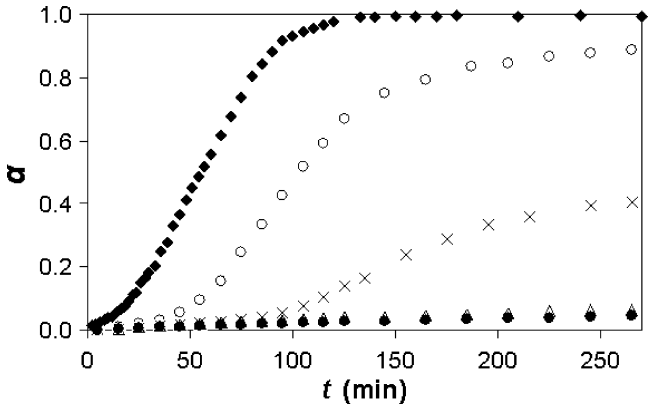

Fig. 9. Effect of Ca^{2+} concentration on the dissolution curves at pH 9 in 10^{-3} M KCl and 25 °C. Ca^{2+} concentrations: diamonds, 0 M; open circles, 3×10^{-5} M; crosses, 1×10^{-4} M; open triangles, 3×10^{-4} M; solid circles, 1×10^{-3} M.

who found that HA solutions (200 mg/L dissolved C) only precipitated when Ca^{2+} concentration was 3×10^{-3} M or higher.

Carboxylate and phenolate groups of HA molecules are known to have a considerable affinity for divalent cations. Kinniburgh et al. [26], for example, showed that Ca^{2+}, Cd^{2+}, Cu^{2+} and others bind these functional groups of HA in the dissolved state. On the other hand, Ghabbour et al. [27,28] showed that functional groups located at the surface of solid HA particles have also important affinity for divalent cation, such as Pb^{2+}, Hg^{2+} and Mn^{2+}. Therefore, it seems that binding of Ca^{2+} at the surface of HA particles is the responsible for the decrease in the dissolution rate shown in Fig. 9. On one side, the binding of these cations to surface molecules should decrease the net negative charge and the electrostatic repulsion among them. On the other side, bound cations could also act as bridges between functional groups of two adjacent molecules increasing the attractive forces between them. Since calcium ions are known to quickly bind HA molecules, Ca^{2+} binding seems to take place along with deprotonation in the first step of the scheme presented in Fig. 8, resulting in an increased attractive interaction and a reduced electrostatic repulsion among the molecules, which ends up with a decreased dissolution rate.

4. Conclusions

The results shown in this article reveal that the dissolution rate of the studied HA is strongly dependent on pH, increasing as pH increases. The dissolution mechanism is believed to be

strongly related to the deprotonation of carboxylic and phenolic functional groups of the HA molecules, which results in the breaking of some hydrogen bonds that hold the HA molecules together in the solid, leaving the molecules more susceptible for detachment. This deprotonation also results in an increased electrostatic repulsion among surface molecules, which may contribute to increase their rate of detachment from the surface.

The dissolution rate at constant pH is also strongly dependent on Ca^{2+} concentration, decreasing as Ca^{2+} concentration increases. These ions are believed to rapidly adsorb at the particle surface decreasing the electrostatic repulsion among HA molecules. Cations could also act as bridges between functional groups of two adjacent molecules increasing the attractive forces between them, contributing to decrease the dissolution rate.

The dissolution rate is also increased by increasing temperature and stirring rate. The apparent activation energy of the process and the effects of stirring rate indicate that there is a mixed-control (surface and transport) of the dissolution kinetics under our experimental conditions.

In spite of the results presented in this article, much work is still needed to achieve a good understanding on how and how fast molecules constituting HS particles leave the particles and pass to the aqueous solution. For example, it is still necessary to understand the shape of the dissolution curves, mainly the initial portion of the curves, where a relatively slow dissolution is observed. As indicated above, hydration of surface molecules could be responsible for this, although other processes may also operate. Since the presence of cations strongly reduce the dissolution rate, it is possible that minute amounts of metallic impurities that result from the extraction of the sample are decreasing the dissolution rate at the beginning of the process. Once part of the HA particles are dissolved, HA molecules in solution will surely complexate the cations decreasing their ability to obstruct dissolution.

Acknowledgments

This work was financed by CONICET and SECYT (Argentina). M. Brigante thanks CONICET for the fellowship granted. The authors thank F. Arce (University of Santiago de Compostela, Spain) and his research group, who kindly provided the HA sample.

References

[1] P. MacCarthy, Soil Sci. 166 (2001) 738.
[2] R. Sutton, G. Sposito, Environ. Sci. Technol. 39 (2005) 9009.
[3] A. Piccolo, Soil Sci. 166 (2001) 810.
[4] L.A. Oste, W.H. Van Riemsdijk, E.J.M. Temminghoff, Environ. Sci. Technol. 36 (2002) 208.
[5] F.J. Stevenson, Geochemistry of soil humic substances, in: G.R. Aiken, D.M. McKnight, R.L. Wershaw, P. MacCarthy (Eds.), Humic Substances in Soil, Sediment, and Water: Geochemistry, Isolation, and Characterization, John Wiley & Sons, New York, 1989, pp. 13–52.
[6] M.H.B. Hayes, Extraction of humic substances from soil, in: G.R. Aiken, D.M. McKnight, R.L. Wershaw, P. MacCarthy (Eds.), Humic Substances in Soil, Sediment, and Water: Geochemistry, Isolation, and Characterization, John Wiley & Sons, New York, 1989, pp. 329–362.
[7] B. Gu, J. Schmitt, Z. Chen, L. Liang, J.F. McCathy, Environ. Sci. Technol. 28 (1994) 38.
[8] M.J. Avena, L.K. Koopal, Environ. Sci. Tecnol. 32 (1998) 2572.
[9] T.H. Yoon, S.B. Johnson, G.E. Gordon Jr., Langmuir 21 (2005) 5002.
[10] J.P. Pinheiro, A.M. Mota, J.M.R. dĭOliveira, J.M.G. Martinho, Anal. Chim. Acta 329 (1996) 15.
[11] M.J. Avena, K.J. Wilkinson, Environ. Sci. Technol. 36 (2002) 5100.
[12] R.A. Alvarez-Puebla, C. Valenzuela-Calahorro, J.J. Garrido, Sci. Total Environ. 353 (2006) 243.
[13] K. Wrobel, B.B.M. Sadi, K. Wrobel, J.R. Castillo, J.A. Caruso, Anal. Chem. 75 (2003) 761.
[14] L. Weng, E.J.M. Temminghoff, W.H. van Riemsdijk, Eur. J. Soil Sci. 53 (2002) 575.
[15] G. Furrer, W. Stumm, Geochim. Cosmochim. Acta 50 (1986) 1847.
[16] W.H. Casey, Encyclopedia Surf. Colloid Sci. (2002) 1486–1495.
[17] A.G.S. Prado, C. Airoldi, Thermochim. Acta 405 (2003) 287.
[18] D. Xu, S. Zhu, H. Chen, F. Li, Colloids Surf. A 276 (2006) 1.
[19] M. Klučáková, M. Pekař, Colloids Surf. A 286 (2006) 126.
[20] G.P. Zanini, M.J. Avena, S. Fiol, F. Arce, Chemosphere 63 (2006) 430.
[21] A. Hocsman, S. Di Nezio, L. Charlet, M. Avena, J. Colloid Interface Sci. 297 (2006) 696.
[22] H. Kipton, J. Powell, R.M. Town, Anal. Chim. Acta 267 (1992) 47.
[23] D.L. Sparks, Kinetics of Soil Chemical Processes, Academic Press, San Diego, 1989.
[24] A.C. Lasaga, Kinetic Theory in the Earth Sciences, Princeton University Press, New Jersey, 1998.
[25] C.J. Milne, D.G. Kinniburgh, E. Tipping, Environ. Sci Technol. 35 (2001) 2049.
[26] D.G. Kinniburgh, W.H. van Riemsdijk, L.K. Koopal, M. Borkovec, M.F. Benedetti, M.J. Avena, Colloids Surf. A 151 (1999) 147.
[27] E.A. Ghabbour, M. Shaker, A. El-Toukhy, I.M. Abid, G. Davies, Chemosphere 63 (2006) 477.
[28] E.A. Ghabbour, M. Shaker, A. El-Toukhy, I.M. Abid, G. Davies, Chemosphere 64 (2006) 826.